Experimental analysis of the pyrolysis of solids exposed to transient irradiation: Applications to ignition criteria

Experimental analysis of the pyrolysis of solids exposed to transient irradiation. Applications to ignition criteria.

Simon Santamaria, Rory M. Hadden*

School of Engineering. The King's Buildings. The University of Edinburgh. Edinburgh, UK. EH9 3DW

Abstract

Ignition and flame spread theory is fundamental for evaluating the risk posed by a material during the early stages of a fire. This paper presents an experimental investigation aimed at understanding the parameters which govern the ignition of solids exposed to transient irradiation. Emphasis is placed on the conditions at ignition, including an energy balance to describe surface phenomena and the link between gas phase and solid phase processes. Experiments were performed in a fire calorimetry apparatus and incorporated a gas analysis system to study gas phase composition. Samples of Polyamide 6 (PA6) measuring $85 \times 85 \times 20$ mm were used. Experiments were carried out to independently measure temperature in the solid phase and mass loss rate (MLR) over time. The MLR at ignition was calculated to be between 2.0 and 6.0 $g/(m^2 \cdot s)$ for all but 3 experiments, were outliers presented values of 7.9, 10.7 and 14.4 $g/(m^2 \cdot s)$. Temperature was recorded through the thickness of the solid, at depths of 4, 8, 12 and 16 mm from the surface. A regression analysis was used to calculate the surface temperature at ignition for all ex-

*Corresponding author:
Email address: R.Hadden@ed.ac.uk (Rory M. Hadden)

periments, and it was found to vary between 270 and 325 °C for all but one experiment, were a temperature of 402 °C was recorded. The temperature distribution in the solid phase was used to estimate the net absorbed heat flux at the surface by applying Fourier's law; with values ranging between 2.0 and 9.8 kW/m^2. From the gas analysis, it was possible to assess the identity, mass flux and concentration of three dominant species produced before ignition: carbon monoxide, methane and hexane. These results are of value for the physical modelling of ignition and flame spread phenomena, allowing for more accurate criteria to describe the onset of ignition under a range of heating conditions.
Keywords: ignition criteria, energy balance, mass balance.

---

1. Introduction

Ignition of solid fuels has been extensively studied [1–5]. The accuracy with which ignition can be predicted is of great significance for the fire science community with implications to flame spread and fire risk. Although emphasis has historically been placed on understanding the pyrolysis of solids exposed to constant Incident Heat Fluxes (IHF), recent studies have investigated the applicability of ignition theory for exposure to transient IHF, including experimental, numerical and analytical approaches [6–10]. This work addresses the pyrolysis of solids exposed to transient IHF and analyses how this boundary condition affects the ignition phenomena. This is of importance for modelling the onset of ignition under realistic scenarios. The transient IHF provides an insight into complex boundary conditions which can be used to test and develop the physical models of ignition with direct

applications to flame spread and fire growth predictions.

Ignition theory aims to predict the onset of gas phase combustion by solving the heat transfer in the solid and specifically at the solid's surface. Gas phase phenomena are explicitly excluded, even though the formation of a flammable mixture is fundamental to the ignition process. Equation 1 presents the time dependent energy balance at the surface, where $\dot{q}_{inc}$ is controlled by the experimental apparatus, $\dot{q}_{net}$ is the Net Heat Flux (NHF) absorbed by the solid and $\dot{q}_{surf}$ groups convective and radiative surface losses.

$$\dot{q}"_{inc} = \dot{q}"_{net} + \dot{q}"_{surf} \tag{1}$$

Past studies have used several assumptions to simplify the numerical solutions when modelling ignition. These include: inert material until ignition, disregarding convective heat losses, disregarding endothermic reactions (e.g. melting or bubbling) [4] and disregarding conductive losses through the back face of the material [2]. This study looks at their validity under transient IHF.

Previous studies have generally not addressed the gas phase phenomena, with the experimental design allowing for simplifying assumptions.

1.1. Ignition Criteria

Current physical models of ignition depend on the definition of a critical parameter or combination of parameters that provide a threshold for the onset of ignition, known as ignition criteria. Different parameters have been used with this purpose, including: critical IHF [1], surface temperature and mass loss rate at ignition [1, 6]. The concept of total incident energy has also been discussed, but has been demonstrated to be inappropriate [6].

The constant surface temperature criteria has been studied extensively [1, 3, 6, 11] and has remained a tacit assumption for the scientific study of ignition [1]. It assumes that a solid has a unique surface temperature at which ignition will occur. However, past studies have shown that materials can ignite over a wide range of surface temperatures [6, 11] and it has been observed that time to ignition is likely to be determined by the material's thermal inertia and not its ignition temperature [1], making it a pseudo-fundamental parameter. Moreover, surface temperature measurements carry high levels of uncertainty as charring, melting, bubbling or shrinkage can affect radiation and thermocouple positioning.

The flux of pyrolysates can be experimentally measured through an assessment of the mass loss rate [12]. This has most notably been developed into fire point theory [5], where an energy balance is used to describe a critical mass flux required for ignition. It identifies three properties related to the fuel that can be used to quantify the ignitability of a material: the heat of combustion of the pyrolysis gases, the heat of pyrolysis of the material and the maximum heat losses that the flame can withstand without being extinguished. The gas phase phenomena are analysed by considering the composition of the gases, which determines the flammability limits and the heat of combustion of the mixture, and the flow field, which defines the convective heat transfer coefficient. Studies have investigated the variability of this parameter under different conditions, such as flow rate, oxygen concentration or IHF [5]. The critical mass loss rate was found to slightly increase with increasing incident heat flux and increasing flow rate.

The characteristics of wood pyrolysis have been shown to differ when

samples are exposed to transient IHF [9]. Time to ignition in a fire calorimetry apparatus was successfully modelled, but these results only apply to a charring solid and the irradiation rates used are an order of magnitude higher than those employed in this study. Ignition under a decreasing transient IHF was studied by [7], where a narrow range of times to ignition was found, meaning that ignition is determined by the maximum IHF and a critical ratio between surface cooling and pyrolysis. The decreasing rate of the IHF determines whether ignition occurs, but it does not affect the time to ignition.

Other authors have put forward the concept of a dual threshold, grouping MLR and surface temperature [6] aimed at characterizing no-ignition scenarios. Although MLR has been shown to provide more exact results when modelling time to ignition, compared to surface temperature, results are highly sensitive to the choice of value used [8], which highlights the importance of investigating the assumption of a constant MLR at ignition as well as the dependence on material properties and experimental set-up. Furthermore, at lower irradiation rates, surface phenomena play a dominant role and characterizing their impact is paramount for improving ignition modelling. This work presents a novel approach to aid in the understanding of the pyrolysis process of a solid when exposed to complicated boundary conditions by calculating the energy balance and evaluating the gas phase composition in real time.

2. Experimental methodology

The material studied was polyamide 6 (PA6), a thermoplastic nylon polymer with a thermal conductivity of 0.29 $W/(m \cdot K)$, density of 1183 g/m^3

and a melting temperature of 220 °C (data provided by the manufacturer). Its flammability properties have been studied previously under conditions of constant heating [13, 14].

Samples were exposed to linearly increasing IHFs. The gradient of this line is defined as the irradiation rate. The IHF was provided by four infrared heaters, containing six tungsten filament tubular quartz lamps [15]. The IHF is controlled by a pre-defined heat flux vs time relationship. The equipment is calibrated using a Schmidt-Boelter heat flux gauge with a response time of 0.25 seconds at the range of measurement used. A calibration is completed before any experimental session and a polynomial fit is used to determine the IHF, where $\dot{q}_{inc} = a \cdot V^2 + b \cdot V + c$, with V the output Voltage to the lamps.

All PA6 samples measured $85 \times 85 \times 20$ mm. The sides of the samples were covered with two layers of non-flammable, ceramic paper (2 mm thickness /each), with a density $\rho = 150\ kg/m^3$ and a melting point of 2000 °C, covered by aluminium foil. The back of the samples were covered with a thin layer of thermal paste to reduce thermal contact resistance, which permits the assumption of negligible contact heat losses; samples are positioned on top of an aluminium block, measuring $90 \times 90 \times 20$ mm, to accommodate for the sample with the insulation. A total of 32 experiments were completed, covering 7 different irradiation rates ($40, 50, 60, 70, 80, 90$ and $100\ W/(m^2 s)$). To avoid interference between mass and temperature measurements, 16 experiments recorded mass loss and 16 in-depth temperature. Experiments exposed to 40 and $100\ W/(m^2 s)$ were repeated twice. All other experiments were repeated once.

2.1. Solid phase measurements

2.1.1. Mass loss and time to ignition

A Metler Toledo load cell model WMS4002-L is used to record the mass loss. The uncertainty is 0.01 g (provided by the manufacturer). A quartz tube is used to enclose the combustion chamber, permitting control over the total inlet volumetric flow, which was set at 0.0017 m^3/s. Ignition is defined as the onset of sustained flaming on the solid's surface. All experiments were recorded with a digital camera and time to ignition measurements were reassessed by video analysis for each test. The uncertainty is estimated at ± 1 s, since the brightness of the lamps interferes with the visual assessment.

2.1.2. In-depth temperatures

Figure 1 shows a diagram of the experimental set-up. Four thermocouples (K type, $\phi = 1$ mm) were positioned inside of the solid to measure the temperature distribution through time, at distances of 4, 8, 12 and 16 mm from the surface. The uncertainty in the thermocouple position is ± 1 mm and the maximum measurement error is 2.5 °C (provided by the manufacturer).

2.2. Gas phase measurements.

A Fourier Transformed Infrared Spectrometer (FTIR) [16] is used to analyse the identity and concentration of the species generated during the pyrolysis process before ignition. The sampling probe is located 900 mm from the sample's surface (see Figure 1). The FTIR provides a semi-quantitative assessment of the components and concentration of the gaseous products. A sampling time of 5 seconds was used. It was estimated that the delay time

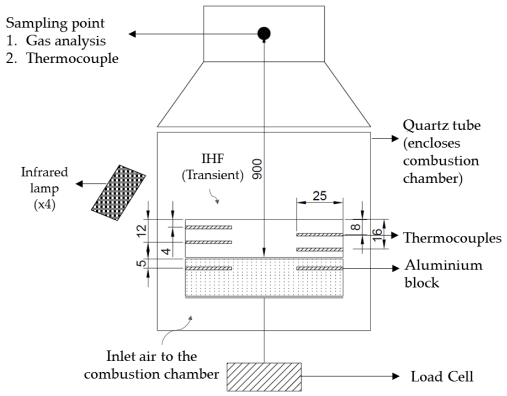

Figure 1: Experimental Set-Up. All dimensions are shown in mm. Figure is not to scale.

associated to mass transport of the gases between the surface and the probe's location is 8 seconds.

PA6 is a thermoplastic polymer formed by carbon, hydrogen, nitrogen and oxygen.The spectrum given by the FTIR analysis was processed to identify the presence and concentration of 14 different species: water vapour, carbon dioxide, carbon monoxide, nitrogen monoxide, nitrous oxide, methane, ethylene, ethane, propane, hexane, butane and pentane. Previous studies have used Thermogravimetric Analysis (TGA) and Evolved Gas Analysis (EGA) to analyse the decomposition of PA6 [14] and results are later used to model the thermal degradation emphasizing the release of NH_3, H_2O, CO_2 and caprolactam. Since the exact conditions of pyrolysis and burning in the TGA are not well characterized, the list of species considered in this study is considered appropriate to provide simplified mass transport and flammability limit measurements.

2.3. Calculation procedures

2.3.1. Mass Loss Rate

A novel methodology is used to calculate the MLR at ignition. MLR is the derivative of the mass loss over time. Due to the low signal to noise ratio, a simple differentiation technique will result in large uncertainty. The traditional methodology [17], uses a five point numerical differentiation equation to smooth the results, which permits analysis during flaming. This is commonly used with HRR measurements to calculate an effective heat of combustion.

However, by smoothing the results, this methodology increases the uncertainty when determining the MLR at a specific time t (e.g. $t_{ignition}$). For this reason a new method is adopted in this study. The mass loss over time is plotted as a scatter graph for each experiment. The analysis centers on a period of 135 seconds, defined as: $t_{ignition} - 90s < t_{ignition} < t_{ignition} + 45s$.

Close to ignition, an increase in the mass loss per unit time can be seen, shown as a steeper negative gradient in the scatter graph. A period is chosen for each experiment where the gradient appears to remain constant, and the data is fitted by a linear fit, where: $mass(t) = a \cdot t + b$. The time interval used varied between 25 s and 40 s, depending on the experimental conditions. The slope of this line (coefficient a) is then used as the $MLR_{ignition}$. The uncertainty associated to the MLR is the 95% confidence interval from the linear fit.

2.3.2. Surface Temperature

A quadratic fit is used to determine the surface temperature at ignition. This method is highly sensitive to the temperature readings at $x = 4mm$

from the surface (T_4). A visual assessment of the temperature profile as determined from the quadratic fit evidenced the impact of uncertainties in the location of T_4. Knowing that the temperature profile must define a concave function, results were the quadratic term was negative were also not considered. This resulted in a total of 9 experiments reported (see Figure 3).

2.3.3. Net Heat Flux

The NHF is calculated by evaluating Fourier's law $\dot{q}_{net} = -k \cdot \frac{dT}{dx}$ at $x = 0$, where $T(x)$ is defined by the quadratic fit. This represents the absorbed energy by the solid at ignition. The thermal conductivity is assumed to be invariant with temperature.

2.3.4. Surface losses

The surface losses are determined using two methodologies and the results are compared. First, from Equation 1, $\dot{q}"_{surf} = \dot{q}"_{inc} - \dot{q}"_{net}$. This is shown in Figure 3. Second, knowing the surface temperature at ignition, T_{surf}, the surface losses can also be calculated as:

$$\dot{q}"_{surf} = \dot{q}"_{conv} + \dot{q}"_{rad} \tag{2}$$

The convective losses are calculated by $\dot{q}"_{conv} = h \cdot (T_{ignition} - T_{ambient})$. Where h, the convective heat transfer coefficient, is calculated as $h = \frac{Nu \cdot k}{L}$, with Nu, the Nusselt number equal to $0.54 \cdot Ra^{1/4}$ and the Rayleigh number $Ra = \frac{g \cdot \beta (T_{ignition} - Tamb)}{\nu \alpha}$. The characteristic length is $L = \frac{A}{P}$, with A the surface area and P the perimeter of the sample. The air is assumed to be at $T_{amb} = 20$ $^{\circ}C$ and the conductivity of air, $k = 0.026$ $W/(m \cdot K)$. Assumptions include constant properties and free convection from an isothermal, horizontal hot

plate [18]. This is supported by previous studies that have shown reduced mixing of the inlet flow to the FPA above the material surface [19].

Radiative losses are calculated by $\dot{q}"_{rad} = \epsilon \cdot \sigma \cdot T^4_{ignition}$, where σ is the Stefan-Boltzman constant: $5.67 \cdot 10^{-}8\ W/(m^2 \cdot K^4)$ and ϵ is the emissivity, assumed 1 [20]. Comparisons between both methods are shown in Figure 4 and discussed in Section 3.

2.3.5. Mass balance and flammability limits

The FTIR reports the concentration in parts per million (ppm). Using the ideal gas law, the mass yield of each species is calculated as shown by Equation 3, where $\dot{V}$ is the volumetric flow of 0.0017 m^3/s, $[Y_i]$ is the concentration of species i at t_i, P is the absolute pressure, MW is the molecular weight of each compound, $R = 8.314\ J/(mol \times K)$ is the universal gas constant and T is the temperature in K.

$$\dot{m_X} = \dot{V} \times \frac{[Y_i]}{10^6} \times \frac{P \times MW}{R \times T} \tag{3}$$

Equation 4 [3] provides an expression to calculate the lower flammability limit (LFL) of a mixture of gases at elevated temperatures, where L_i is the LFL of each component and P_i is the concentration of each species. The mean gas phase temperature at ignition at the probe location is 100 °C ± 20 °C. Temperatures at the location of the pilot are expected to be higher.

$$L_T = \frac{100}{\sum \frac{P_i}{L_i}}(1 - 7.8 \cdot 10^{-4}(T - 25)) \tag{4}$$

3. Results and Discussion

Figure 2 shows the time to ignition (mean values) for all experiments. For irradiation rates of 40 and 100 $W/(m^2 \cdot s)$, each marker represents the average for 6 experiments; for all others, 4. Since standard deviation $< 1\%$ for all irradiation rates, the uncertainty is not shown in the figure. As the irradiation rate increases, the time to ignition decreases, approaching an asymptote. This is expected since for higher irradiation rates ignition will be governed by the material properties.

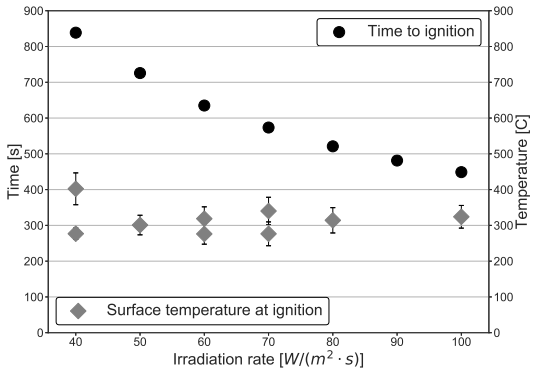

Figure 2: Time to ignition (mean) and Surface Temperature at ignition.

As explained in Section 2.3.2, only 9 experiments are shown for results that depend on the quadratic fit for the temperature profile (Surface Temperature, NHF and Surface Losses). Surface temperatures seem to remain constant. However, for lower irradiation rates, it was seen that surface and bubbling phenomena played a significant role. Bubbling of PA6 has an impact on the heat and mass transfer processes. During experiments at 40 and 50 $W/(m^2 \cdot s)$, bubbles resulted from the accumulation of pyrolysis gases inside of a superficial skin developed on the material's surface. These bubbles

would occupy between 30% and 60% (approximately) of the sample's surface and could remain without bursting for periods of up to 10 seconds. The accumulation clearly impacts the mass transport of pyrolysates as well as the flow structure and mixture fraction. Furthermore, the space between the bubble and the solid would effectively insulate the sample, reducing the absorption of energy. For this reason, the uncertainty of the surface temperature increases with lower irradiation rates.

Figure 3 shows the NHF (Fourier's law) and Surface Losses (Equation 1). The values at the top of each bar represents the IHF at ignition (sum of NHF and Surface Losses). Although extreme values of 2.3 and 9.8 kW/m^2 for the NHF were recorded, this can be explained by higher uncertainties at lower irradiation rates. The mean uncertainty for the NHF is 1.6 kW/m^2, with a standard deviation (of the uncertainty) of 0.3 kW/m^2. This means that the uncertainty in the NHF is constant for all irradiation rates and it is not shown in Figure 3 for clarity. A mean of 6.4 ± 2.3 kW/m^2 is reported, which modifies to 6.5 ± 1.6 kW/m^2 if results at the lowest heating rate are not considered. The energy flux term associated to the production of pyrolysates ($\dot{q}_{pyr}$) is a fraction of the NHF, since the latter includes conductive losses through the back boundary as well as other endothermic reactions (bubbling, melting, etc). Understanding the variation of the NHF with the irradiation rates is essential for accurately describing the onset of ignition, since it provides insight into the effects of the transient IHF on the production of pyrolysates. Furthermore, future studies focusing on the evolution of this term with time (and not only at ignition) can reveal the relation between the impact of boundary conditions and the material's thermal properties.

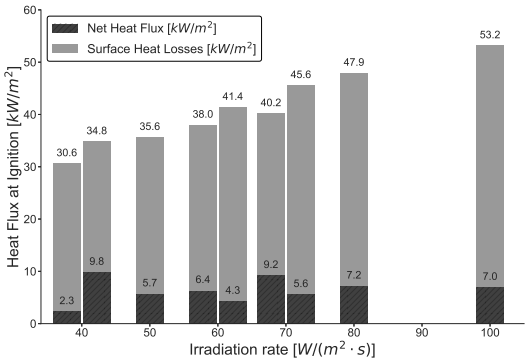

Figure 3: NHF (Fourier's law), Surface Losses (Eq. 1) and IHF at ignition.

The concept of the critical IHF defines a thermal state in the sample where the rate of heat losses (through all boundaries) equals the NHF. If a transient IHF is defined, a steady state situation will not be reached and the specific value of a critical IHF can not be defined. However, a critical ratio between the surface losses and the IHF from the sample will determine whether or not ignition can occur. From Figure 3, this ratio ($Losses_{ignition}/IHF_{ignition}$) is $84 \pm 6\%$. Values of the instantaneous IHF at ignition reported in this study are much higher than critical values of 12-17 kW/m^2 reported in [12] or 20 kW/m^2 reported in [14] for the ignition of PA6. Those studies, however, exposed samples to constant IHF.

Figure 4 shows the results of calculating the NHF from Equation 1 after determining the surface losses from Equation 2. The temperature gradient becomes steeper close to the surface, meaning that values shown in Figure 3 underestimate the NHF. However, the losses shown in Figure 4 are also determined from the surface temperatures estimated by a quadratic fit. Since this value is also underestimated, radiative losses will be much larger, reducing the NHF. Although not explicitly shown, convective losses using this method

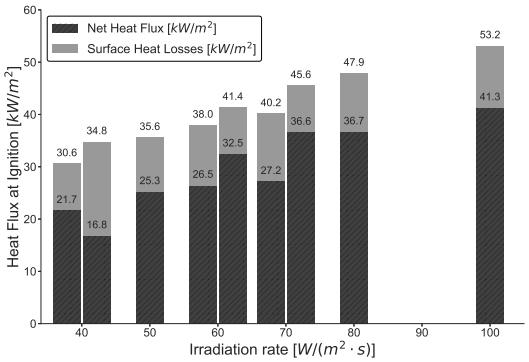

Figure 4: NHF (Eq. 1), Surface Losses (Eq. 2) and IHF at ignition.

account for 34% - 42% of the total losses, which challenges the validity of the assumption of disregarding surface convective losses. At higher surface temperatures, radiative losses will dominate since the temperature dependence is to the fourth power, but most likely, for lower irradiation rates in transient IHF, convective losses play a considerable role.

Figure 5 shows $MLR_{ignition}$. A mean value of 5.31 ± 3.27 $g/(m^2 s)$ can be reported. Without considering the two outliers at 50 $W/(m^2 s)$ and 60 $W/(m^2 s)$, a value of 4.27 ± 1.57 $g/(m^2 s)$ is found. The $MLR_{ignition}$ seems to increase slightly with the irradiation rate, until it reaches a maximum value at 70 $W/(m^2 s)$, after which a small reduction takes place, however large scatter in the data precludes a definite statement. These values are smaller than those obtained by [14], where a mean of 6.5 $g/(m^2 s)$ is reported although [12] reported a value of 3 $g/(m^2 s)$ for ignition of PA6. Both studies used constant IHF.

Surface bubbling at lower irradiation rates affects the release of pyrolysis gases. It is possible that the bubble allows accumulation of gases to take place and because of that, a lower instantaneous $MLR_{ignition}$ may be measured

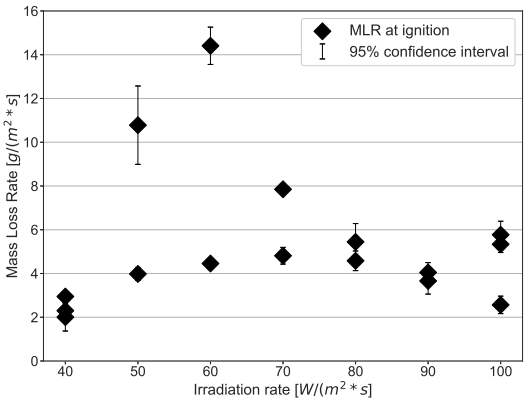

Figure 5: Mass loss rate (MLR) at ignition.

since mixing and transport to the pilot only takes place when the bubble bursts, releasing accumulated gases. As the heating rate increases, bubbling becomes less significant and so accumulation plays a lesser role. However, for higher heating rates, ignition will take place at higher IHF, and so, the higher energy absorption by the flammable gases and the higher flow temperatures could be responsible for the slight decrease in the required mass flux of gases, since at higher temperatures the lower flammability limit (LFL) will decrease [3] and lower concentrations may ignite.

Figure 6 shows the concentration in parts per million (ppm) for the three dominant species (CO, CH_4 and C_6H_{14}). These were identified by evaluating the concentration of all species mentioned in Section 2.2. Both maximum concentrations in the experimental period and overall ratio with the other compounds were considered. As shown in Figure 1, the temperature was recorded at the location of the probe. Using Equation 3, the mass yield of each species is calculated. This data is used to assess the flammable mixture that forms on top of the surface before ignition. The mean gas

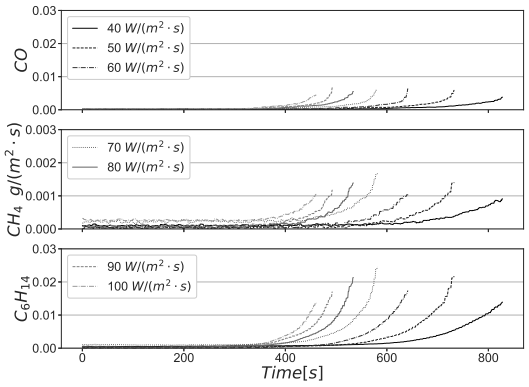

Figure 6: Mean mass flux of carbon monoxide, methane and hexane. To preserve the detail, the abscissa for methane is an order of magnitude smaller.

phase temperature at ignition at the probe location is 100 °C ± 20 °C. Temperatures at the location of the pilot are expected to be higher.

Using Equation 4, the LFL for the mixture at ignition is calculated. This is shown in Figure 7. Concentrations at the probe are two orders of magnitude lower. Since the flammable mixture is attained, as ignition was recorded, the difference in concentration can be explained by the dilution of the gases due to mixing with the inlet flow, as well as undetected gases by the FTIR. Previous studies [19] have shown that only a small fraction of inlet flow of the FPA interacts with the gases on top of the sample. If this fraction is within the range of 0.25 - 0.4 % then the concentration will be at the LFL. A detailed study of the flow inside of the FPA combustion chamber needs to be made to accurately evaluate gas mixing. These results highlight the complexities associated to evaluating the gas phase phenomena at ignition. Species concentrations need to be measure at the pilot's location, which raises challenges associated to absorption and obstruction of the IHF, as well as affecting the

flow.

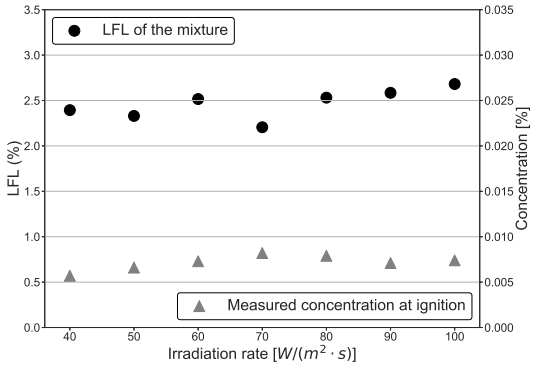

Figure 7: Lower Flammability Limit (LFL) and experimental concentration of the mixture (FTIR).

4. Conclusions

This paper has investigated the ignition of Polyamide 6 samples when exposed to transient IHF. An energy balance was used where the surface defines the control volume to facilitate a comparison between the energy absorbed and the losses at the surface. Under constant IHF, the concept of a critical IHF is based on the attainment of a steady state where the surface losses equal the IHF. This concept can't be extended to transient IHF, but a ratio between the surface losses and the IHF at ignition is investigated for all experimental conditions and was shown to be $84 \pm 6\%$.

In-depth temperature measurements were used to perform a quadratic fit and determine the surface temperature. At lower irradiation rates, the uncertainty increases as the bubbling phenomena dominates. Surface temperature at ignition was shown to increase slightly with the irradiation rate. For higher irradiation rates, the time to ignition approaches an asymptote,

as faster heating rates result in material properties dominating the response.

The variability of the NHF was investigated using two similar methodologies. Since both of them rely on the quadratic fit for the temperature profile, the importance of surface phenomena was highlighted as bubbling and melting increase the uncertainty. The applicability of surface temperature as an ignition criteria has been questioned as this has been shown to vary with experimental conditions. For thermoplastic solids exposed to transient IHF with low irradiation rates, an accurate measurement of the surface temperature (or an accurate definition of the surface) will prove challenging. Commonly used assumptions (inert solid and negligible convective losses) are discussed and it is shown that endothermic surface processes (e.g. bubbling) cannot be neglected.

The mean $MLR_{ignition}$ was found to be 5.31 ± 3.27 $g/(m^2s)$, although this value was reduced to 4.27 ± 1.57 $g/(m^2s)$ if outliers are removed. This compares to values of 3 $g/(m^2s)$ and 6.5 $g/(m^2s)$ previously reported in the literature for constant IHF. The $MLR_{ignition}$ initially increases as bubbling (and subsequent bursting) at lower irradiation rates result in sudden releases of pyrolysates. For higher irradiation rates, the $MLR_{ignition}$ decreases. This is attributed to higher surface temperatures, higher flow temperatures and lower flammable limits.

The total yield of three dominant gas phase species was calculated. It was found that only a fraction of the mass lost rate is represented, showing that the three species studied are not sufficient to describe the thermal degradation of the solid. The attainment of the LFL was investigated and the dilution of the inlet flow analysed to evaluate the concentration of the

mixture at the solid surface. This work furthers the study of heating under transient irradiation and demonstrates that presently the only approach that can be relied upon to predict ignition is a full energy balance on the solid coupled with detailed understanding of the gas phase phenomena.

5. Acknowledgements

Funding from the BRE Trust and the University of Edinburgh is gratefully acknowledged.

References

[1] V. Babrauskas, Ignition HandBook, Society of Fire Protection Engineers, 2003, pp. 234–352.

[2] J. Torero, Flaming ignition of solid fuels, SFPE Handbook of Fire Protection Engineering, 5th (2016) 631–661.

[3] D. Drysdale, An Introduction to Fire Dynamics, John Wiley & Sons, Ltd, 2011, pp. 181–223.

[4] C. Lautenberger, A. Fernandez-Pello, Approximate analytical solutions for the transient mass loss rate and piloted ignition time of a radiatively heated solid in the high heat flux limit, Fire Safety Science 8 (2005) 445–456.

[5] D. J. Rasbash, D. D. Drysdale, D. Deepak, Critical heat and mass transfer at pilot ignition and extinction of a material, Fire Safety Journal 10 (1) (1986) 1–10.

[6] I. Vermesi, N. Roenner, P. Pironi, R. M. Hadden, G. Rein, Pyrolysis and ignition of a polymer by transient irradiation, Combustion and Flame 163 (2016) 31 – 41.

[7] R. Bilbao, J. F. Mastral, J. A. Lana, J. Ceamanos, M. E. Aldea, M. Betrn, A model for the prediction of the thermal degradation and ignition of wood under constant and variable heat flux, Journal of Analytical and Applied Pyrolysis 62 (1) (2002) 63 – 82.

[8] J. Gong, Y. Li, Y. Chen, J. Li, X. Wang, J. Jiang, Z. Wang, J. Wang, Approximate analytical solutions for transient mass flux and ignition time of solid combustibles exposed to time-varying heat flux, Fuel 211 (2018) 676 – 687.

[9] Y. Lizhong, G. Zaifu, Z. Yupeng, F. Weicheng, The influence of different external heating ways on pyrolysis and spontaneous ignition of some woods, Journal of Analytical and Applied Pyrolysis 78 (1) (2007) 40 – 45.

[10] C. Zhai, J. Gong, X. Zhou, F. Peng, L. Yang, Pyrolysis and spontaneous ignition of wood under time-dependent heat flux, Journal of Analytical and Applied Pyrolysis 125 (2017) 100 – 108.

[11] H. Thomson, D. Drysdale, C. Beyler", An experimental evaluation of critical surface temperature as a criterion for piloted ignition of solid fuels, Fire Safety Journal 13 (2) (1988) 185 – 196.

[12] R. E. Lyon, J. G. Quintiere, Criteria for piloted ignition of combustible solids, Combustion and Flame 151 (4) (2007) 551 – 559.

[13] R. Carvel, T. Steinhaus, G. Rein, J. L. Torero, Determination of the flammability properties of polymeric materials: A novel method, Polymer Degradation and Stability 96 (3) (2011) 314–319.

[14] T. Steinhaus, Determination of intrinsic material flammability properties from material tests assisted by numerical modelling, Phd (2009).

[15] ASTM, Standard test methods for measurement of material flammability using a fire propagation apparatus (fpa) (2013).

[16] A. A. Stec, P. Fardell, P. Blomqvist, L. Bustamante-Valencia, L. Saragoza, E. Guillaume, Quantification of fire gases by ftir: Experimental characterisation of calibration systems, Fire Safety Journal 46 (5) (2011) 225 – 233.

[17] ISO, Reaction-to-fire tests – heat release, smoke production and mass loss rate – part 1: Heat release rate (cone calorimeter method) (2002).

[18] F. P. Incropera, Fundamentals of Heat and Mass Transfer, John Wiley and Sons, Inc., USA, 2006.

[19] R. Hadden, Smouldering and self-sustaining reactions in solids: an experimental approach, Phd (2011).

[20] J. Zhang, M. A. Delichatsios, S. Bourbigot, Experimental and numerical study of the effects of nanoparticles on pyrolysis of a polyamide 6 (pa6) nanocomposite in the cone calorimeter, Combustion and Flame 156 (11) (2009) 2056 – 2062.